Analysis on the Frumkin Adsorption Isotherm of the Over-Potentially Deposited Hydrogen (OPD H) at the Polycrystalline Ni | Alkaline Aqueous Electrolyte Interface Using the Phase-Shift Method

Jang H. Chun* and Sang K. Jeon

Mission Technology Research Center, Department of Electronic Engineering, Kwangwoon University, Seoul 139-701, Korea
(Received August 6, 2001 : Accepted October 5, 2001)

Abstract : The Frumkin adsorption isotherm of the over-potentially deposited hydrogen (OPD H) for the cathodic H_2 evolution reaction (HER) at the poly-Ni|0.05 M KOH aqueous electrolyte interface has been studied using the phase-shift method. The behavior of the phase shift $(0° \leq -\phi \leq 90°)$ for the optimum intermediate frequency corresponds well to that of the fractional surface coverage $(1 \geq \theta \geq 0)$ at the interface. The phase-shift method, i.e., the phase-shift profile $(-\phi$ vs. $E)$ for the optimum intermediate frequency, can be used as a new method to estimate the Frumkin adsorption isotherm $(\theta$ vs. $E)$ of the OPD H for the cathodic HER at the interface. At the poly-Ni|0.05 M KOH aqueous electrolyte interface, the rate (r) of change of the standard free energy of the OPD H with θ, the interaction parameter (g) for the Frumkin adsorption isotherm, the equilibrium constant (K) for the OPD H with θ, and the standard free energy (ΔG_θ) of the OPD H with θ are 24.8 kJ mol^{-1}, 10, $5.9 \times 10^{-6} \leq K \leq 0.13$, and $5.1 \leq \Delta G_\theta \leq 29.8$ kJ mol^{-1}, respectively. The electrode kinetic parameters $(r, g, K, \Delta G_\theta)$ depend strongly on θ $(0 \leq \theta \leq 1)$.

초 록 : 위상이동 방법을 이용하여 다결정 Ni|0.05 M KOH 수용액 계면에서 음극 H_2발생 반응을 위한 과전위 전착 (흡착)된 수소의 Frumkin 흡착등온식을 연구조사 하였다. 다결정 Ni|0.05 M KOH 수용액 계면에서, 최적중간주파수일 때 위상이동$(0° \leq -\phi \leq 90°)$ 거동은 표면피복율$(1 \geq \theta \geq 0)$ 거동에 정확하게 상응한다. 최적중간주파수일 때 위상이동 변화 $(-\phi$ vs. $E)$ 즉 위상이동 방법은 다결정 Ni|0.05 M KOH 수용액 계면에서 음극 H_2발생 반응을 위한 과전위 전착(흡착)된 수소의 Frumkin 흡착등온식$(\theta$ vs. $E)$을 추정할 수 있는 새로운 방법으로 사용될 수 있다. 다결정 Ni|0.05 M KOH 수용액 계면에서, 표면피복율에 따른 과전위 전착(흡착)된 수소의 표준자유에너지 변화율(r), Frumkin 흡착등온식 의 상호작용 파라미터(g), 표면피복율(θ)에 따른 과전위 전착(흡착)된 수소의 흡착평형상수(K)와 표준자유에너지(ΔG_θ)는 각각 24.8 kJ mol^{-1}, 10, $5.9 \times 10^{-6} \leq K \leq 0.13$, $5.1 \leq \Delta G_\theta \leq 29.8$ kJ mol^{-1} 이다. 전극속도론적 파라미터$(r, g, K, \Delta G_\theta)$ 는 표면피복율(θ)에 따른다.

Key words : Phase-shift method; Frumkin adsorption isotherm; Over-potentially deposited hydrogen; Nickel electrode

1. Introduction

Nickel is the most frequently used for the catalytic hydrogenation processes. Also, nickel is the most widely used as cathodes and activated cathodes to produce H_2 in alkaline aqueous electrolytes.[1-3] The kinetics and mechanisms of the cathodic H_2 evolution reaction (HER) at Ni | alkaline aqueous electrolyte interfaces have been intensively studied in interfacial electrochemistry.[4-10]

Many electrochemical methods and analyses on the H adsorption sites and processes for the cathodic HER at Ni | alkaline aqueous electrolyte interfaces are described and reviewed elsewhere.[6-8,10] The cyclic voltammetric and electrochemical impedance spectroscopic methods have been extensively used to study the cathodic HER at the interfaces. However, it seems to be that the phase-shift profile for the optimum intermediate frequency has not been used to study the H adsorption sites and processes, i.e., the Frumkin

adsorption isotherms, at the Ni | alkaline aqueous electrolyte interfaces.

The relation, transition, and criterion of the under-potentially deposited hydrogen (UPD H) and the over-potentially deposited hydrogen (OPD H) are necessary and important to understand the kinetics and mechanisms of the cathodic HER at the interfaces. It is well known that the UPD H and the OPD H occupy different surface adsorption sites and act as two distinguishable electroadsorbed H species while only the OPD H can contribute to the cathodic HER.[4,11-16]

The Frumkin adsorption isotherm is based on the kinetics and thermodynamics of the electrode interfaces. It is well known that the Langmuir adsorption isotherm is a special case of the Frumkin adsorption isotherm. The Langmuir adsorption isotherm can be derived from the Frumkin adsorption isotherm by setting the interaction parameter is zero. Although both the Frumkin and Langmuir adsorption isotherms may be regarded a classical model and theory in physical electrochemistry,[17] it is useful and effective to study the H adsorption sites and processes for the cathodic HER at

the interfaces. Thus, there is a need in the art for a fast, simple, and reliable technique to estimate or determine the Frumkin adsorption isotherms for characterizing the OPD H for the cathodic HER at the Ni | alkaline aqueous electrolyte interfaces.

Recently, we have experimentally and consistently found that the phase-shift profile for the optimum intermediate frequency, i.e., the phase-shift method, can be effectively used to estimate the Langmuir or the Frumkin adsorption isotherms of the UPD H and the OPD H for the cathodic HER at the interfaces.[18-21] Although the proposition of the phase-shift method is not based on the kinetics or the thermodynamics, it is useful for studying the OPD H for the cathodic HER at the poly-Ni | alkaline aqueous electrolyte interfaces.

In this paper we will represent the Frumkin adsorption isotherm of the OPD H for the cathodic HER at the poly-Ni | 0.05 M KOH aqueous electrolyte interface using the phase-shift method. It is complementary to the Langmuir adsorption isotherm of the OPD H for the cathodic HER at the poly-Au | 0.5 M H_2SO_4 aqueous electrolyte interface.[23] It appears that the phase-shift method is useful and effective to estimate or determine the Frumkin adsorption isotherm as well as the Langmuir adsorption isotherm. Also, it is useful and effective to study the kinetics and mechanisms of the OPD H for the cathodic HER at iron group (Fe, Co, Ni) | alkaline aqueous electrolyte interfaces.

2. Experimental

2.1. Preparations

Taking into account H^+ concentrations and effects of pH,[22] an alkaline aqueous electrolyte was prepared from KOH (Alfa Aesar, Johnson Matthey, purity: 99.995%) with purified water (resistivity: > 18 MΩ cm) obtained from a Millipore system. The 0.05 M KOH aqueous electrolyte was deaerated with 99.999% purified nitrogen gas for 10 min before the experiments.

A standard 3-electrode configuration was employed using an SCE reference electrode and a poly-Ni foil (Johnson Matthey, purity: 99.994%, surface area: ~10.4 cm^2) working electrode. The poly-Ni foil was polished with alumina powder (0.3 and 0.05 μm) to a mirror-like finish. The polished poly-Ni foil was rinsed with the Millipore Milli-Q water using an ultrasonic bath. A Pt wire (Johnson Matthey, purity: 99.95%, 1.5 mm diameter) was used as a counter electrode. The working and counter electrodes were separately placed (~4 cm) in the same compartment Pyrex cell using Teflon holders.

2.2. Measurements

Cyclic voltammetric (scan potential: 0 to -1.20 V vs. SCE, scan rate: 200 mV s^{-1}) and ac impedance (single sine wave, scan frequency: 10^4 to 1 Hz, ac amplitude: 5 mV, dc potential: 0 to -1.40 V vs. SCE) techniques were used to study the relation between the phase-shift profile for the optimum intermediate frequency and the corresponding Frumkin adsorption isotherm.

The cyclic voltammetric experiment was performed using an EG&G PAR Model 273A potentiostat controlled with the PAR Model 270 software package. The ac impedance experiment was performed using the same apparatus in conjunction with a Schlumberger SI 1255 HF Frequency Response Analyzer controlled with the PAR Model 388 software package. In order to obtain comparable and reproducible results, all measurements were carried out using the same preparations, procedures, and conditions at room temperature. The international sign convention is used, i.e., cathodic currents and lagged phase shifts or angles are taken as negative.

3. Results and Discussion

3.1. Cyclic voltammogram

Fig. 1 shows the cyclic voltammogram of the steady state at the poly-Ni | 0.05 M KOH aqueous electrolyte interface. The H desorption peak occurs at ca. -0.66 V vs. SCE. In contrast to the poly-Pt interfaces, the UPD H peaks are not observed at the poly-Ni interface.[15,16] It implies that the Frumkin adsorption isotherm of the UPD H for the cathodic HER is not experimentally observable.

3.2. Phase-shift profile for the optimum intermediate frequency

The equivalent circuit for the cathodic HER is usually expressed as shown in Fig. 2(a). Practically, the relaxation time effect on the ac impedance experiment must be considered at the poly Ni | 0.05 M KOH aqueous electrolyte interface. Therefore, the equivalent circuit elements shown in Fig. 2(a) should be defined as: R_S is the electrolyte resistance, R_F is the equivalent circuit element of the faradaic resistance (R_ϕ) for the discharge reaction, R_P is the equivalent circuit element of the faradaic resistance for the recombination reaction, C_P is the equivalent circuit element of the adsorption pseudocapacitance (C_ϕ), and C_D is the double-layer capacitance. The two equivalent circuit elements, i.e., R_F and C_P, are the equivalent resistance and capacitance associated with the
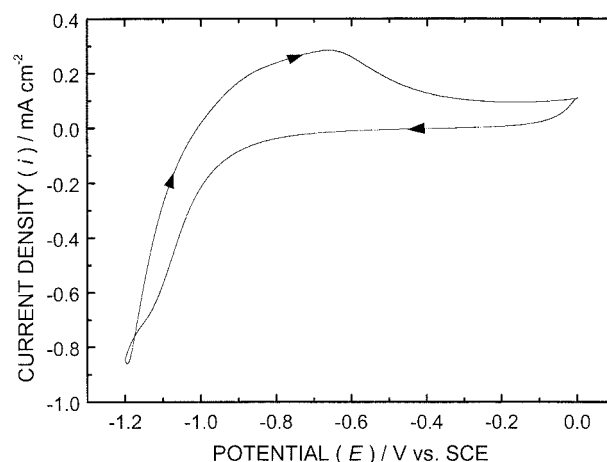

Fig. 1. The typical cyclic voltammogram at the poly-Ni | 0.05 M KOH aqueous electrolyte interface. Surface area: ~10.4 cm^2. Scan potential: 0 to -1.20 V vs. SCE. Scan rate: 200 mV s^{-1}. 20th scan.
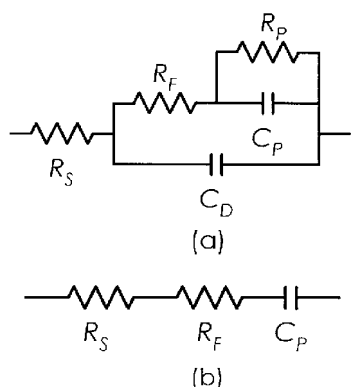
Fig. 2. (a) The equivalent circuit for the cathodic H_2 evolution reaction at the poly-Ni | 0.05 M KOH aqueous electrolyte interface and (b) The simplified equivalent circuit for the intermediate frequencies at the interface.
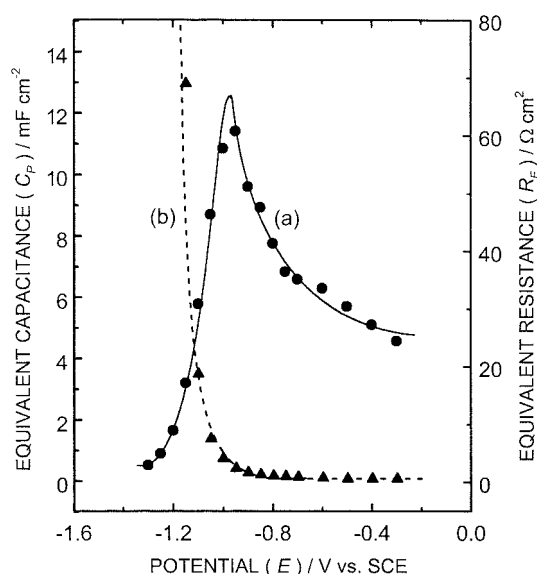

Fig. 3. The profiles of the measured equivalent circuit elements (R_F, C_P) respect to E for the optimum intermediate frequency (ca. 4 Hz) at the poly-Ni | 0.05 M KOH aqueous electrolyte interface. Single sine wave. Scan frequency: 10^4 to 1 Hz. ac amplitude: 5 mV. dc potential: -0.10 to -1.35 V vs. SCE. (a) Equivalent resistance (R_F) and (b) Equivalent capacitance (C_P).

adsorption processes of H, respectively.

At intermediate frequencies, the equivalent circuit can be simplified as a serial connection of R_S, R_F, and C_P shown in Fig. 2(b). Since, practically, C_P is much greater than C_D. However, it implies that the simplified equivalent circuit for the intermediate frequencies can be applied to the poly-Ni | 0.05 M KOH aqueous electrolyte interface regardless of H_2 evolution. In other words, it is valid and effective for studying the UPD H and/or the OPD H at the interface. This is described in more detail elsewhere.[21,23]

Under the Frumkin adsorption conditions, the phase shift or angle (ϕ) corresponding to the equivalent circuit for the intermediate frequencies shown in Fig. 2(b) can be derived as follows[19-21,23]:

$$\phi = -\tan^{-1}[1/\omega(R_S + R_F)C_P] \tag{1}$$

$$R_F \propto R_\phi \ (< \ R_\phi) \ \text{and} \ C_P \propto C_\phi \ (> \ C_\phi) \tag{2}$$

$$C_\phi = (\gamma F/RT)\theta(1 - \theta)/[1 + g\theta(1 - \theta)] \tag{3}$$

$$g \equiv r/RT \tag{4}$$

where $\omega \ (= 2\pi f)$ is the angular frequency, R_ϕ is the faradaic resistance for the discharge reaction of the UPD H or the OPD H, C_ϕ is the adsorption pseudocapacitance for the Frumkin adsorption conditions, γ is the charge corresponding to the saturation coverage of θ, θ is the fractional surface coverage of the UPD H or the OPD H, F is the Faraday constant, R is the gas constant, T is the absolute temperature, g is the interaction parameter for the Frumkin adsorption isotherm, and r is the rate of change of the standard free energy of the UPD H or the OPD H with θ. A minus sign shown in Eq. (1) implies a lagged phase. From Eq. (1), it is readily understood that the lagged phase depends strongly on R_F and C_P, i.e., R_ϕ and C_ϕ or θ. In other words, the phase shift (-ϕ) depends markedly on the adsorption processes of the UPD H and/or the OPD H at the interface.

Figs. 3(a) and (b) show the profiles of the measured R_F and C_P respect to E for the optimum intermediate frequency (ca. 4 Hz) at the poly-Ni | 0.05 M KOH aqueous electrolyte

interface, respectively. The two profiles of R_F and C_P shown in Fig. 3 are similar to those at the poly-Au | 0.5 M H_2SO_4 aqueous electrolyte interface.[23] The significant difference between the profiles of R_F is related to the two different adsorption processes, i.e., the Frumkin adsorption process at the poly-Ni | 0.05 M KOH and the Langmuir adsorption process at the poly-Au | 0.5 M H_2SO_4 aqueous electrolyte interface. As shown in Fig. 3(a), the profile of R_F due to the Frumkin adsorption process is much broader than that due to the Langmuir adsorption process. It is attributed to the interaction parameter (g). However, the behavior of the phase shift ($0° \leq -\phi \leq 90°$) for the optimum intermediate frequency can be related to that of the fractional surface coverage ($1 \geq \theta \geq 0$). In other words, the change rate of $\Delta(-\phi)/\Delta E$ or $d(-\phi)/dE$ corresponds well to that of $\Delta\theta/\Delta E$ or $d\theta/dE$. This is discussed in more detail later.

Fig. 4 shows the comparison of the two extremely distinguishable frequency responses at the poly-Ni | 0.05 M KOH aqueous electrolyte interface. The absolute value of the impedance vs. the frequency ($|Z|$ vs. f) is plotted on a log-log scale. In Fig. 4(a), the slope portion of the frequency response curve represents the capacitive behavior of the interface. Since, a slope of -1 represents the ideal capacitive behavior. It implies that C_P has a minimum value as shown in Fig. 3(b). It also implies that θ can be set zero as shown in Table 1. Therefore, from Eq. (1), -ϕ has a maximum value ($\leq 90°$) as shown in Fig. 5(a) and Table 1. On the other hand, in Fig. 4(b), the horizontal portion of the frequency response curve represents the resistive behavior of the interface. Since, a slope of zero represents the ideal resistive behavior. It implies that the H adsorption at the interface is almost saturated. In other words, C_P has a maximum value as shown in
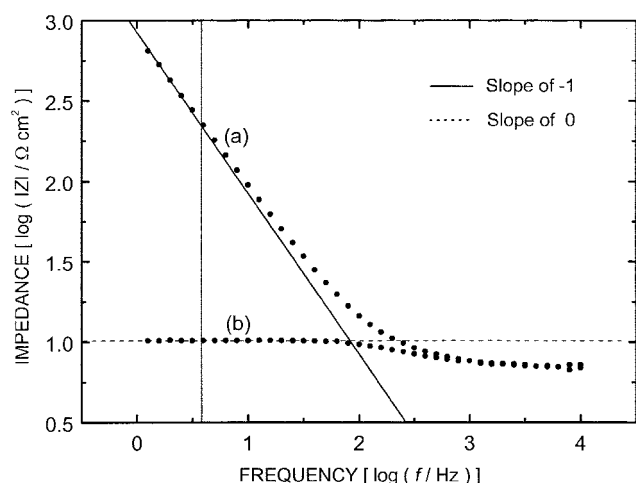
Fig. 4. The comparison of the two extremely distinguishable frequency response curves at the poly-Ni | 0.05 M KOH aqueous electrolyte interface. Vertical solid line: ca. 4 Hz. Single sine wave. Scan frequency: 10^4 to 1 Hz. ac amplitude: 5 mV. dc potential: (a) -0.30 V and (b) -1.30 V vs. SCE.
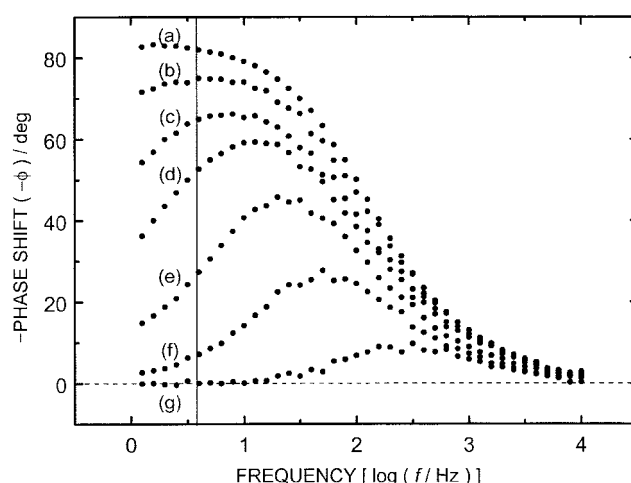

Fig. 5. The comparison of the phase-shift curves at the poly-Ni | 0.05 M KOH aqueous electrolyte interface. Vertical solid line: ca. 4 Hz. Single sine wave. Scan frequency: 10^4 to 1 Hz. ac amplitude: 5 mV. dc potential: (a) -0.30 V, (b) -0.80 V, (c) -0.90 V, (d) -0.95 V, (e) -1.05 V, (f) -1.15 V, and (g) -1.30 V vs. SCE.

Table 1. The measured phase shift (-ϕ) for the optimum intermediate frequency (ca. 4 Hz) and the estimated fractional coverage (θ) at the poly-Ni | 0.05 M KOH aqueous electrolyte interface

E (V vs. SCE)	-ϕ (deg)	θ^a
-0.40	81.2	≈ 0
-0.50	80.8	0.005
-0.60	80.2	0.012
-0.70	78.7	0.031
-0.75	77.6	0.044
-0.80	75.0	0.076
-0.85	70.5	0.132
-0.90	64.9	0.201
-0.95	52.6	0.352
-1.00	38.0	0.532
-1.05	27.3	0.664
-1.10	16.4	0.798
-1.15	7.2	0.911
-1.20	2.4	0.970
-1.25	0.7	0.991
-1.30	0	≈ 1

^{a}Estimated using the measured phase shift (-ϕ).

Fig. 6. The phase-shift profile (-ϕ vs. E) for the optimum intermediate frequency (ca. 4 Hz) at the poly-Ni | 0.05 M KOH aqueous electrolyte interface.

Fig. 3(b). It implies that θ can be set unity as shown in Table 1. Therefore, from Eq. (1), -ϕ has a minimum value ($\geq 0°$) as shown in Fig. 5(g) and Table 1.

Fig. 5 shows the comparison of the phase-shift curves (-ϕ vs. f) for the different cathode potentials at the poly-Ni | 0.05 M KOH aqueous electrolyte interface. In Fig. 5, as expected, the phase-shift curves and phase angles are markedly characterized at the intermediate frequencies. The low side (ca. 4 Hz) of a slope of -1 shown in Fig. 4(a), i.e., the low side of the intermediate frequ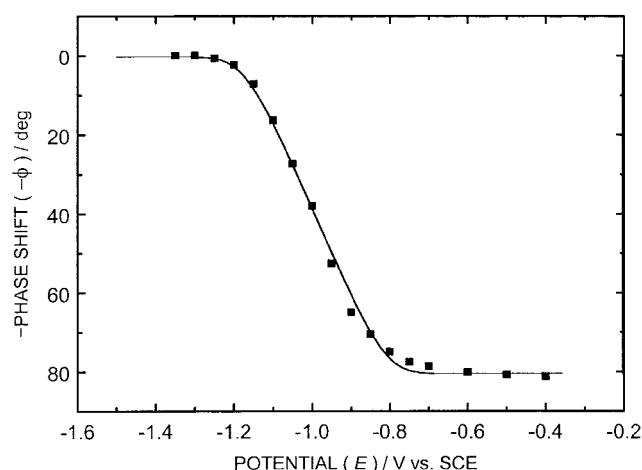encies (ca. 1 to 10 Hz), can be set as the optimum intermediate frequency for the phase-shift profile (-ϕ vs. E). Of course, the exactly same phase-shift profile can also be obtained at ca. 1 and 10 Hz, i.e., the range of the intermediate frequencies. The determination of the optimum intermediate frequency for the phase-shift profile is described elsewhere.[18-21,23,24]

Finally, the cathode potentials and the corresponding phase shifts for the optimum intermediate frequency (ca. 4 Hz) can be plotted as the phase-shift profile (-ϕ vs. E) shown in Fig. 6. As expected, the phase-shift profile (-ϕ vs. E) due to the Frumkin adsorption process varies more slowly than that due to the Langmuir adsorption process. It is attributed to the interaction parameter (g) of the Frumkin adsorption process.

Fig. 7 shows the comparison of the change rates of the -ϕ vs. E and the θ vs. E, i.e., the Δ(-ϕ)/ΔE or d(-ϕ)/dE and the $\Delta\theta/\Delta E$ or $d\theta/dE$, at the poly-Ni | 0.05 M KOH aqueous elec-
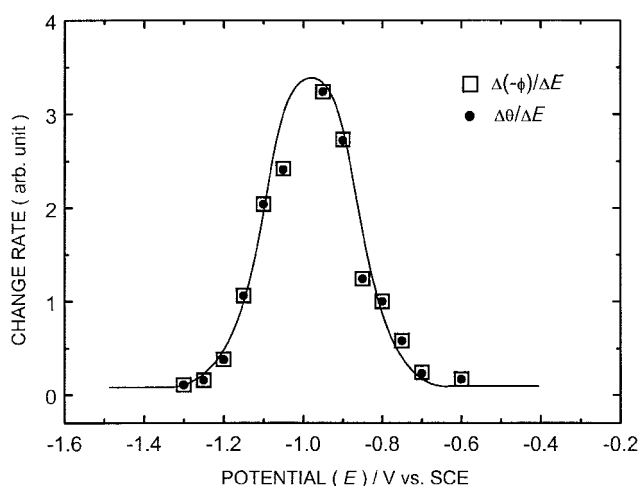
Fig. 7. The comparison of the change rates of the $\Delta(-\phi)/\Delta E$ and the $\Delta\theta/\Delta E$ for the optimum intermediate frequency (ca. 4 Hz) at the poly-Ni | 0.05 M KOH aqueous electrolyte interface.

Fig. 8. The comparison of the experimental and fitted data for the Frumkin adsorption isotherm (θ vs. E) at the poly-Ni | 0.05 M KOH aqueous electrolyte interface. $K_o = 0.13$ and $g = 10$.

trolyte interface. The shape of the change rates is much broader than that due to the Langmuir adsorption process. As previously described, it is attributed to the interaction parameter (g) of the Frumkin adsorption process. Fig. 7 also shows that the $\Delta(-\phi)/\Delta E$ or $d(-\phi)/dE$ corresponds well to the $\Delta\theta/\Delta E$ or $d\theta/dE$ regardless of the Frumkin or the Langmuir adsorption process. It implies that the behavior of the phase shift ($0^o \leq -\phi \leq 90^o$) corresponds well to that of the fractional surface coverage ($1 \geq \theta \geq 0$) under the Frumkin adsorption conditions as well as the Langmuir adsorption conditions. The derivation and interpretation of the change rates are described elsewhere.[19-21,23]

3.3. Frumkin adsorption isotherm

The Frumkin adsorption isotherm is based on the assumptions that the surface is inhomogeneous and that lateral interaction effects are not negligible. Considering the application of the Frumkin adsorption isotherm to the formation of H on the poly-Ni surface, the Frumkin adsorption isotherm can be expressed as follows[25]:

$$[\theta/(1 - \theta)]\exp(g\theta) = K_O C_{H^+}[\exp(-EF/RT)] \qquad (5)$$

where θ is the fractional surface coverage of the UPD H or the OPD H, K_O is the equilibrium constant for the UPD H or the OPD H at $g = 0$, C_{H^+} is the H$^+$ concentration in the bulk electrolyte, E is the applied dc potential, i.e., the cathode potential, F is the Faraday constant, R is the gas constant, and T is the absolute temperature. In Eq. (5), $g = 0$ corresponds to the Langmuir adsorption isotherm.

At the poly-Ni | 0.05 M KOH aqueous electrolyte (pH 13.7) interface, the fitted data, i.e., the calculated Frumkin adsorption isotherm using Eq. (5), are shown in Fig. 8. As expected, the Frumkin adsorption isotherm (θ vs. E) shown in Fig. 8 corresponds well to the phase-shift profile ($-\phi$ vs. E) for the optimum intermediate frequency (ca. 4 Hz) shown in Fig. 6. From Fig. 8, it can be easily inferred that $K_O = 0.13$ and
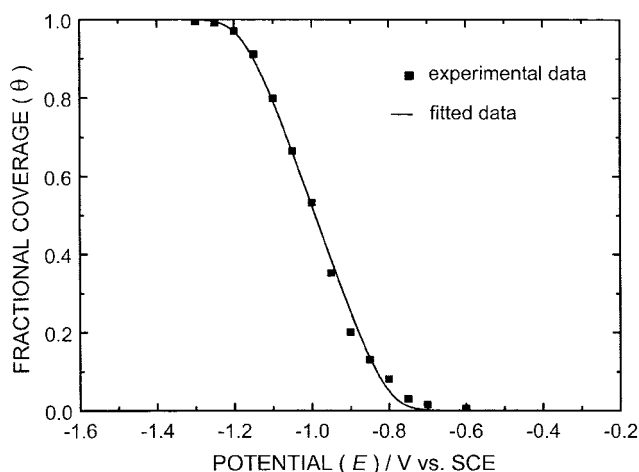
$g = 10$ are applicable to the formation of H at the interface. From Eq. (4), it is readily calculated that r is 24.8 kJ mol^{-1} for $g = 10$. Taking into account a range of 20-60 kJ mol^{-1} for Ni electrodes,[25] 24.8 kJ mol^{-1} can be considered to be reasonable.

The Frumkin adsorption isotherm shown in Fig. 8 is attributed to the OPD H. It should be noted that the Frumkin adsorption isotherm shown in Fig. 8 is located beyond the H desorption peak potential (ca. -0.66 V vs. SCE) shown in Fig. 1. However, as expected, the Frumkin adsorption isotherm due to the UPD H is not observed at the cathode potential range. Since, the oxide-film formation on the poly-Ni surface inhibits the UPD H at the cathode potential range.[1-4,7-10]

Under the Frumkin adsorption conditions, the relation between the equilibrium constant (K) for the OPD H and the standard free energy (ΔG_θ) of the OPD H with θ is given using,[25] as

$$2.3RT \log K = -\Delta G_\theta \qquad (6)$$

$$K = K_O \exp(-g\theta) \qquad (7)$$

At the poly-Ni | 0.05 M KOH aqueous electrolyte interface, it is readily calculated using Eqs. (6) and (7) that ΔG_θ is 5.1 $\leq \Delta G_\theta \leq 29.8$ kJ mol^{-1} for $0.13 \geq K \geq 5.9 \times 10^{-6}$, i.e., $0 \leq \theta \leq 1$. As expected, in contrast to the Langmuir adsorption isotherm, both K and ΔG_θ depend strongly on θ.

Fig. 9 shows the numerically calculated Frumkin adsorption isotherms (θ vs. E) corresponding to the different values of $g = 0$, 10, and 20. In Eqs. (4), (5), (7), and Fig. 9, as previously described, $g = 0$ or $r = 0$ corresponds to the Langmuir adsorption isotherm. However, as g increases, θ increases more slowly with increasing E as shown in Fig. 9.

4. Conclusions

The simplified equivalent circuit for the optimum intermediate frequency and the corresponding phase-shift equation are well fitted to the poly-Ni | 0.05 M KOH aqueous electro-
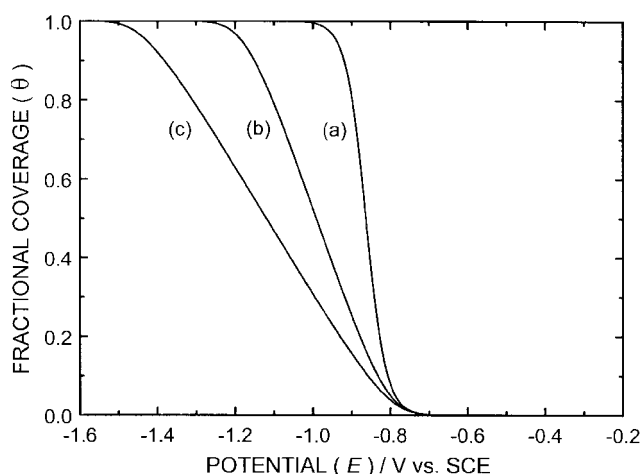
Fig. 9. The numerically calculated Frumkin adsorption isotherm (θ vs. E) at the poly-Ni | 0.05 M KOH aqueous electrolyte interface. (a) $g = 0$ (Langmuir adsorption isotherm), (b) $g = 10$, and (c) $g = 20$.

lyte interface regardless of H_2 evolution. The behavior of the phase shift ($0° \leq -\phi \leq 90°$) for the optimum intermediate frequency corresponds well to that of the fractional surface coverage ($1 \geq \theta \geq 0$) at the interface. The phase-shift profile ($-\phi$ vs. E) for the optimum intermediate frequency, i.e., the phase-shift method, can be used as a new method to estimate the Frumkin adsorption isotherm (θ vs. E) of the OPD H for the cathodic HER at the interface. At the poly-Ni | 0.05 M KOH aqueous electrolyte interface, the rate (r) of change of the standard free energy (ΔG_θ) of the OPD H with θ, the interaction parameter (g) for the Frumkin adsorption isotherm, the equilibrium constant (K) for the OPD H, and the standard free energy (ΔG_θ) of the OPD H with θ are 24.8 kJ mol^{-1}, 10, $5.9 \times 10^{-6} \leq K \leq 0.13$, and $5.1 \leq \Delta G_\theta \leq 29.8$ kJ mol^{-1}, respectively. The electrode kinetic parameters (r, g, K, ΔG_θ) depend strongly on θ ($0 \leq \theta \leq 1$).

References

1. Y. Fukai, "The Metal-Hydrogen System", Springer-Verlag, New York (1993).
2. G. A. Somorjai, "Introduction to Surface Chemistry and Catalysis",
Wiley-Interscience, New York (1994).
3. B. E. Conway, G. Jerkiewicz, Editors, "Electrochemistry and Materials Science of Cathodic Hydrogen Absorption and Adsorption", **PV 94-21**, The Electrochem. Soc., Pennington, NJ (1995).
4. S. Maximovitch, R. Durand, *J. Electroanal. Chem.* **149**, 273 (1983).
5. R. Sandoval, R. Schrebler, H. Gomez, *J. Electroanal. Chem.* **210**, 287 (1986).
6. A. Lasia, A. Rami, *J. Electroanal. Chem.* **294**, 123 (1990).
7. A. Lasia, "Electrochemistry and Materials Science of Cathodic Hydrogen Absorption and Adsorption", B. E. Conway, G. Jerkiewicz, Editors, **PV 94-21**, 261, The Electrochem. Soc., Pennington, NJ (1995).
8. G. Barral, S. Maximovitch, F. Njanjo-Eyoke, *Electrochim. Acta,* **41**, 1305 (1996).
9. S. Maximovitch, *Electrochim. Acta,* **41**, 2761 (1996).
10. M. Bernardini, N. Comisso, G. Mengoli, L. Sinico, *J. Electroanal. Chem.* **457**, 205 (1998).
11. G. Jerkiewicz, *Prog. Surf. Sci.* **57**, 137 (1998).
12. G. Jerkiewicz, A. Zolfaghari, "Electrochemistry and Materials Science of Cathodic Hydrogen Absorption and Adsorption", B. E. Conway, G. Jerkiewicz, Editors, **PV 94-21**, 31, The Electrochem. Soc., Pennington, NJ (1995).
13. G. Jerkiewicz, P. Marcus, Editors, "Electrochemical Surface Science of Hydrogen Adsorption and Absorption", **PV 97-16**, The Electrochem. Soc., Pennington, NJ (1997).
14. A. Zolfaghari, G. Jerkiewicz, *J. Electroanal. Chem.* **467**, 177 (1999).
15. B. E. Conway, G. Jerkiewicz, *Electrochim. Acta.* **45**, 4075 (2000).
16. B. E. Conway, G. Jerkiewicz, "Hydrogen at Surfaces and Interfaces", G. Jerkiewicz, J. M. Feliu, B. N. Popov, Editors, **PV 2000-16**, 1, The Electrochem. Soc., Pennington, NJ (2000).
17. E. Gileadi, In "Electrosorption", E. Gileadi, Editor, pp. 1-18, Plenum, New York (1967).
18. J. H. Chun, K. H. Ra, *J. Electrochem. Soc.* **145**, 3794 (1998).
19. J. H. Chun, K. H. Ra, In "Hydrogen at Surfaces and Interfaces", G. Jerkiewicz, J. M. Feliu, B. N. Popov, Editors, **PV 2000-16**, 159, The Electrochem. Soc., Pennington, NJ (2000).
20. J. H. Chun, S. K. Jeon, *J. Korean Electrochem. Soc.* **4**, 14 (2001).
21. J. H. Chun, K. H. Ra, N. Y. Kim, *Int. J. Hydrogen Energy,* **26**, 941 (2001).
22. E. Gileadi, E. Kirowa-Eisner, J. Penciner, "Interfacial Electrochemistry", 72, Addison-Wesley Pub. Co., Reading, MA (1975).
23. J. H. Chun, S. K. Jeon, *J. Korean Electrochem. Soc.* **4**, 118 (2001).
24. J. H. Chun, K. H. Mun, C. D. Cho, *J. Korean Electrochem. Soc.* **3**, 25 (2000).
25. E. Gileadi, "Electrode Kinetics", 261, VCH, New York (1993).